

Article

Evaluation of Slope Stability Considering the Preservation of the General Patrimonial Cemetery of Guayaquil, Ecuador

Fernando Morante ^{1,2,*}, Maribel Aguilar ^{2,3}, Gonzalo Ramírez ^{2,3}, Roberto Blanco ^{2,4},
Paúl Carrión ^{2,3,*}, Josué Briones ² and Edgar Berrezueta ⁵ 

¹ Facultad de Ciencias Naturales y Matemáticas (FCNM), Geo-recursos y Aplicaciones GIGA, ESPOL Polytechnic University, Escuela Superior Politécnica del Litoral, ESPOL, Campus Gustavo Galindo Km 30.5 Vía Perimetral, P.O. Box 09-01-5863, Guayaquil, Ecuador

² Centro de Investigaciones y Proyectos Aplicados a las Ciencias de la Tierra (CIPAT), ESPOL Polytechnic University, Escuela Superior Politécnica del Litoral, ESPOL, Campus Gustavo Galindo Km 30.5 Vía Perimetral, P.O. Box 09-01-5863, Guayaquil, Ecuador; maesagui@espol.edu.ec (M.A.); goanrami@espol.edu.ec (G.R.); rblanco@espol.edu.ec (R.B.); briones@espol.edu.ec (J.B.)

³ Facultad de Ingeniería Ciencias de la Tierra (FICT), ESPOL Polytechnic University, Escuela Superior Politécnica del Litoral, ESPOL, Campus Gustavo Galindo Km 30.5 Vía Perimetral, P.O. Box 09-01-5863, Guayaquil, Ecuador

⁴ Facultad de Geología y Minas, Instituto Superior Minero Metalúrgico (ISMM), Avenida Calixto García 15, 83300 Moa, Cuba

⁵ Instituto Geológico y Minero de España (IGME), C/Matemático Pedrayes 25, 33005 Oviedo, Spain; e.berrezueta@igme.es

* Correspondence: fmorante@espol.edu.ec (F.M.); pcarrion@espol.edu.ec (P.C.); Tel.: +593-98-829-2937 (F.M.); +593-99-826-5290 (P.C.)

Received: 29 December 2018; Accepted: 20 February 2019; Published: 26 February 2019



Abstract: Inefficient blasting techniques and poor closure management of the old quarry that existed during the 1970s in the area of the actual General Patrimonial Cemetery of Guayaquil resulted in an almost vertical slope of approximately 50 m in height and an intense induced fracturing that weakened the rock mass. This led to the loss of stability and increased material detachment, which damaged the infrastructure of the graveyard representing a risk to visitors and workers. The aim of this research is to evaluate the slope stability through a geotechnical analysis that allows decision-making to recover and preserve the safety of the area. In this work, we used structural measurements and observations made in the field, as well as a three-dimensional model of the slant generated by photographs taken by a drone. Slope Mass Rating (SMR) and Chinese Slope Mass Rating (CSMR) rankings were used to evaluate stability, susceptibility to rockfall was determined using a theoretical–practical procedure, and the safety factor was calculated using the Morgenstern–Price method. The analysis of the geomechanical classifications yielded a low stability value of the slope, which was in accordance with the high susceptibility to rockfall and with the low safety factor. Based on these results, we recommend the application of systematic bolt and shotcrete for stabilization.

Keywords: detachment susceptibility; geomechanical characteristics; CSMR; slope stability; SMR

1. Introduction.

A slope is an inclined surface, often present on geological structures of the earth [1]. The slopes can be formed naturally or, as in the studied case, can be the result of anthropic activity [2]. Slopes and mass movements associated with them are considered geological environmental threats [3].

The stability of a slope is affected by geological, hydrogeological, and geometric factors; topographic conditions; and the geomechanical behavior of the ground [4,5]. The weight of the rocks and the water saturation are two decisive factors in the stability of a rock mass [6]. According to [1], stability is a safety parameter that can be explained as the ability of a land mass to maintain its structure without failing or moving. It can be described by a safety factor [7], which is also a requirement for stabilization intervention recommendations.

The object of the present study is the General Patrimonial Cemetery of Guayaquil. Important people have been buried here, including war heroes, presidents, and artists, who contributed to the development of the country [8]. In 2003, the cemetery was declared Cultural Patrimony of the Nation [9].

The graveyard was expanded and partly built over a scarp left behind by the municipal quarry that operated here during the 1970s.

The basting methods used in the former quarry created an almost vertical slope and induced a series of fractures in the massif that weakened the whole scarp over time, increasing its instability and resulting in the detachment of material. Rockfalls have occurred in the escarpment that have damaged the infrastructure of the Patrimonial Cemetery, such as mausoleums, niches, sculptures, and other buildings, which characterize this heritage of Ecuadorian culture. This also affected the moral and spiritual values of the graveyard.

Considering the unstable conditions of the escarpment located within the cemetery (Gate 1), this study aims at (i) the geomechanical characterization of sedimentary rocks in the studied area (Cemetery of Guayaquil) and (ii) the assessment of the value of data (stability, susceptibility to detachment, and safety factor) obtained from outcrop samples for the estimation of slope stability. Therefore, this paper provides an overview of the process and the results of a characterization methodology that can serve as a basis for more detailed and specific studies of slope stability in similar cases.

2. Geographical and Geological Environment

The study area is located in the declivity of the General Patrimonial Cemetery of Guayaquil, which is at the foot of the escarpment of Cerro del Carmen, facing Julián Coronel street, entering through Gate 1 (Figure 1). The cemetery covers an area of approximately 130,000 m² and the slope where we worked is around 50 m high.

The geological formations underlying Guayaquil are described below in order of age, from the oldest to the youngest:

The Piñón Formation, which, according to [10], is an Upper-Albian–Aptian formation, consists mainly of aphanitic basalts with a pad structure and siliceous shale intercalations in the vicinity of Guayaquil.

The Calentura Formation, of Cenomanian–Upper-Turonian age, is composed of a sequence of gray limestone and calcareous lapilli tuffs with tuffaceous shales in the upper part [11].

The Cayo Formation, of Turonian–Conician age [12], is made up of a rhythmic stratification of tuff shales, lapilli tuff, volcanoclastic agglomerates, and gaps of a greenish color [13,14]. The upper part is altered by spherical weathering and contains grayish-beige tuffaceous shales, tuff, and silicified siltstone [15].

The Maastrichtian Guayaquil formation crops out in the study area [12]. In the lower part, it presents silicified shales and chert nodules alternating with brown-colored tuffaceous siltstones [16], while the upper part consists of sandstones with calcareous cement and silicified shales. There is an abundance of fossil remains [17].

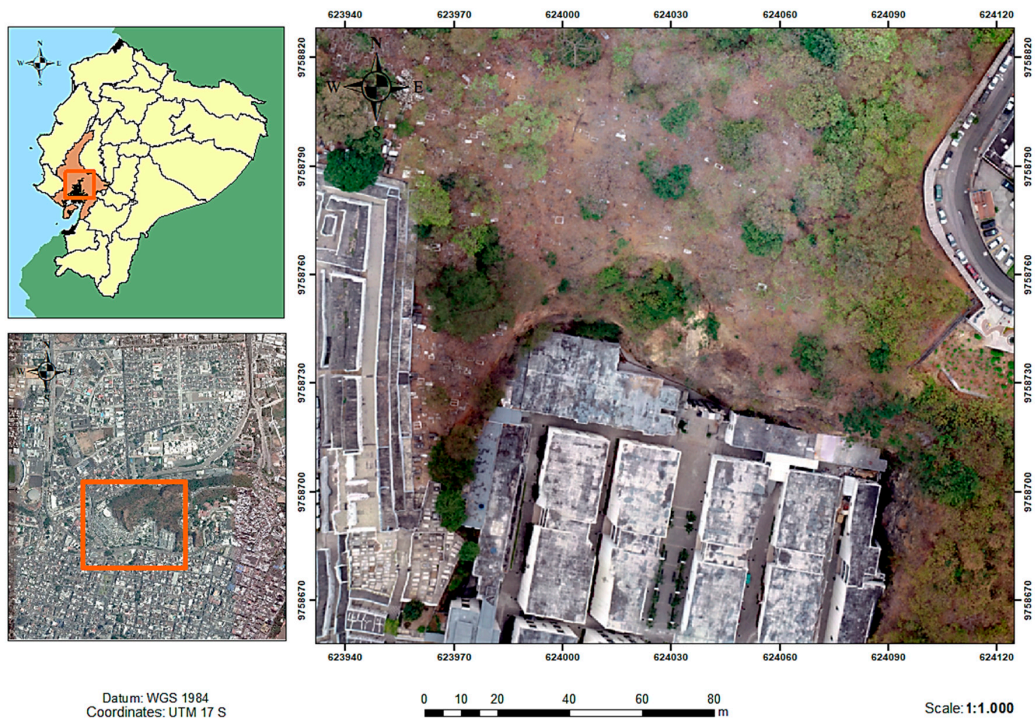


Figure 1. Location map of the study area.

3. Methodology

In order to reach our scientific goals, we followed a methodology that combined experimental work (both in situ and in laboratory) with a series of interpretive activities (Figure 2) which was developed in the following three phases:

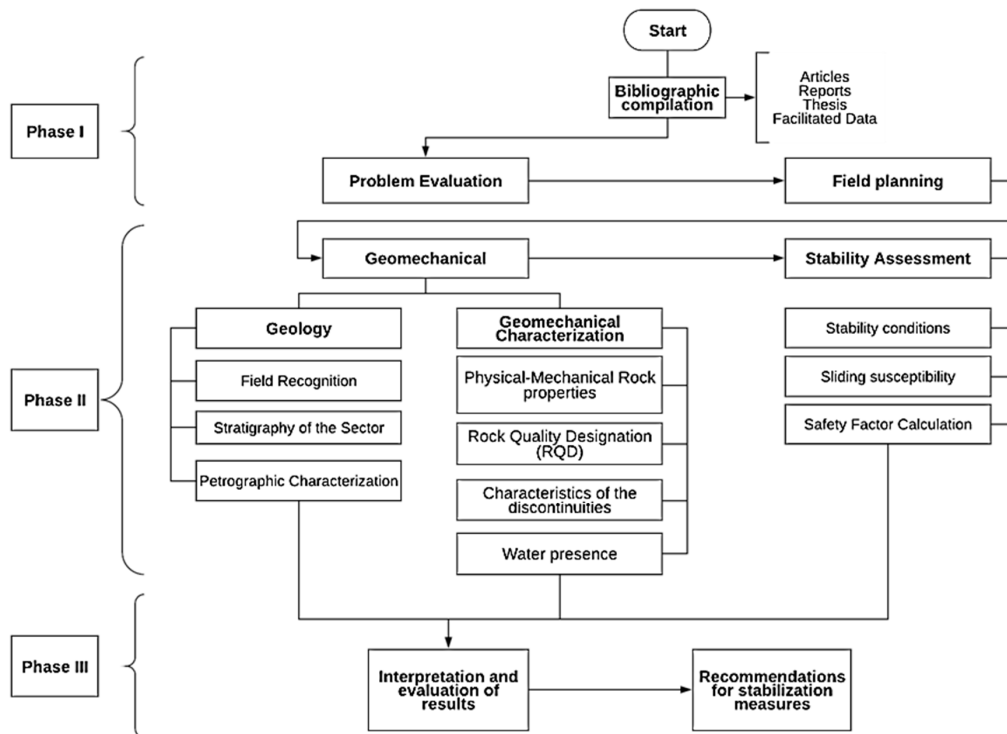


Figure 2. Flowchart of the methodology used in this study.

3.1. First Phase

As a first step, we compiled the relevant bibliography, including articles, reports, and even projects that had been developed in the area, as well as data provided by the “Studies and Proposals for the Stabilization of the Slope in Cerro del Carmen of the General Cemetery (Julián Coronel Street)” project [18]. The literature survey also covered topography, laboratory tests for rocks and soils, and images obtained by a high-resolution drone. In addition, we analyzed the technical and social context considering the causes and the impact of the problem, which helped us assess its importance.

3.2. Second Phase

3.2.1. Geology

Field work in the General Patrimonial Cemetery of Guayaquil allowed us to study the morphology of the terrain and to obtain strike and dip measurements of the slope, the strata, and the fractures. A representative stratigraphic column was constructed based on the lithological observations, and six samples were taken for their description and laboratory tests to assess physical and mechanical properties.

3.2.2. Geomechanical Characterization

Physical–Mechanical Properties

According to [19,20], rocks, such as shale, mudstone, sandstone, slate, gneiss, schist, coal, and marl, present anisotropic mechanical behavior, and these anisotropic rocks usually play an important role in rock engineering. Therefore, the assessment of mechanical properties (such as compressive, shear, tensile, and fracture behavior) provides crucial information for the study of slope stability.

The physical–mechanical properties are necessary to develop the Slope Mass Rating (SMR) and Chinese Slope Mass Rating (CSMR) methods in order to determine the stability conditions. These properties are also required for the calculation of the safety factor (SF).

Simple linear compression, resistance, density, cohesion, and internal friction angle were measured on the six samples. All tests were performed by a specialized rock mechanics laboratory.

The linear resistance to compression was determined by the “standard” method using cores with a 1.5 height/diameter ratio, while for the tensile strength, the “Brazilian test” method was used. According to [21,22], the Brazilian test is a simple indirect testing method to obtain the tensile strength of brittle material such as concrete, rock, and rocklike materials, in which a thin circular disc is diametrically compressed to failure.

Cohesion and angle of internal friction values were established using circles of Mohr–Coulomb stresses from compressive and tensile strength values, using our own data verified by the results of other works.

Rock Quality Designation (RQD)

According to [23,24], the RQD is a modified core recovery percentage, in which all pieces of sound core over 100 mm (4 in.) long are summed and divided by the length of the core run. The RQD index is an index of rock quality “in that problematic rock that is highly weathered, soft, fractures, sheared and jointed is counted against the rock mass” [24].

For field observations, we applied the Priest–Hudson method [25] (Table 1), which takes into account the number of fractures per meter and uses the following formula:

$$\text{RQD} = 100 \times e(-0.1\lambda) \times (0.1\lambda + 1) \quad (1)$$

where λ is the average number of discontinuities per meter.

Table 1. Rock quality designation (RQD) quantitative rating (source: [24]).

RQD (%)	Rock Quality
25	Very Poor
25–50	Poor
50–75	Fair
75–90	Good
90–100	Very Good

Characteristics of Discontinuities

In soils and rocks, discontinuities act as planes of weakness or as conduits of groundwater flow. These features, according to [26,27], can facilitate movements.

The characteristics of discontinuities were determined by a combination of measurements taken during the field trips and the analysis of high-resolution pictures captured by drone. We assessed:

- the separation between diaclasses, which is the average distance between existing fractures in the different sectors of the slope, and
- the state of joints, based on the photographs of the slope acquired with a drone and through in situ observations considering the length of the discontinuity, its opening, roughness, filling, and alteration.

Presence of Water

According to [27,28] the presence of water generally decreases the shear strength of slope-forming material and thereby increases the probability of slope failure. Since it is difficult to assess subsurface flow of groundwater quantitatively, we used visual estimation of field conditions to award the ratings.

The presence of water in the massif was corroborated during field trips, in which dry and wet sectors and sectors with flowing water were differentiated.

3.2.3. Geomechanical Characterization

A three-dimensional model of the slope was generated (Figures 3–5) using photographs taken by a drone. The massif was divided into three zones based on the change in the dip and dip direction, and each zone was divided into sectors (Figures 3 and 6), identifying the main families of discontinuities.

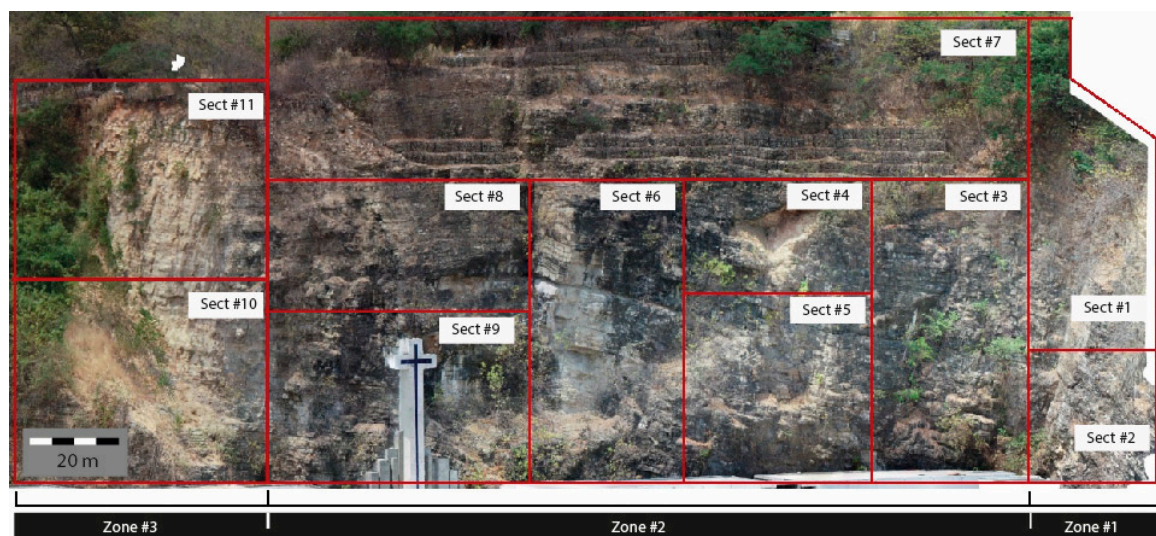


Figure 3. Frontal view of the 3D model of the slope. Division of the slope into zones and sectors.

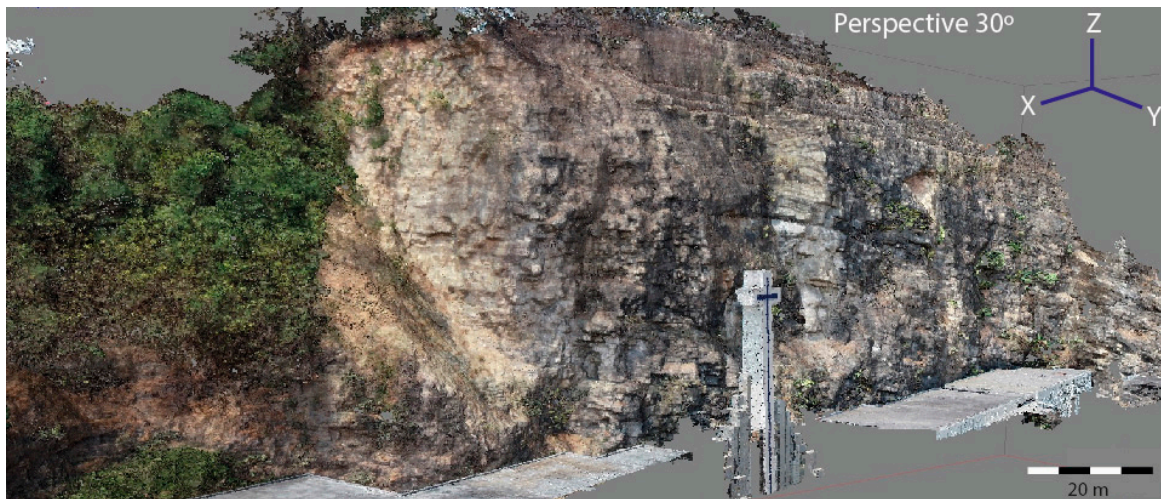


Figure 4. Left view of the 3D model.

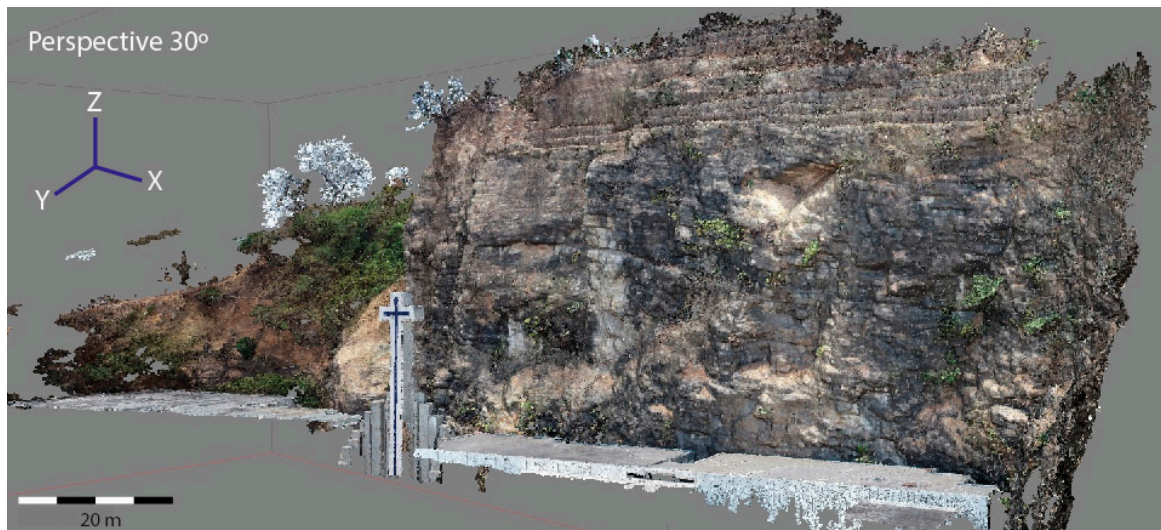


Figure 5. Right view of the 3D model.

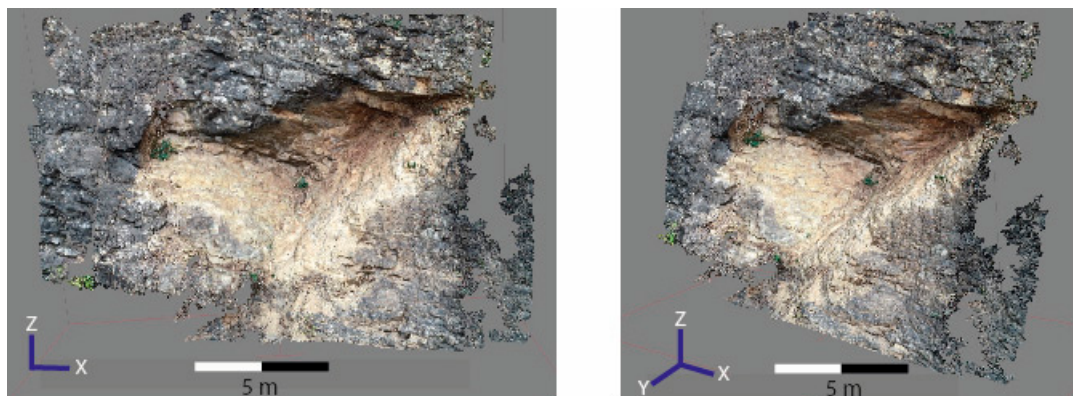


Figure 6. Front and right views of Sector 4.

Based on the geomechanical classifications, we first evaluated the stability conditions in the studied sectors; then, we assessed the susceptibility to detachment; and finally, we determined the safety factor in the profiles that were considered the most critical of each sector.

Stability Conditions

The SMR classifications by Romana [29] and the CSMR classification proposed by [30] were used for the analysis of stability conditions.

We decided to apply the SMR method because of its extensive use in stability assessment studies and also because it provides the basis for the CSMR method, which was deemed necessary due to the height of the scarp.

SMR

The SMR classification was originally published by [29], and it was improved in 1995 [31]. In 2001, correction factors were added to it (as detailed in [32]), and the Rock Mass Rating (RMR) classification, developed for tunnels [33], was adopted by [31] to be applied to slopes. The method is described in Table 2.

The SMR classifies the rocks by their stability, suggesting recommendations of support or corrections of problems (Table 3). To obtain the SMR, an “adjustment factor” (resulting from the multiplication of three subfactors (F_1 , F_2 , and F_3)) and an “excavation factor” (F_4) must be added to the RMR:

$$SMR = RMR + (F_1 \times F_2 \times F_3) + F_4 \tag{2}$$

where F_1 is determined by the degree of parallelism between the strike of the discontinuities and the strike of the slope. It can be adjusted by the following expression:

$$F_1 = (1 - \sin(\alpha_j - \alpha_s))^2 \tag{3}$$

where α_j is the direction of dip of the joints, and α_s is the direction of the slope.

Table 2. Geomechanical classification: RMR and quality of the rock mass (modified from [5,33]).

1	Rock Matrix Resistance (MPa)	Point Load Test	>10	10–4	4–2	2–1	Simple Compression		
		Simple Compression	>250	250–100	100–50	50–25	25–5	5–1	<1
		Score	15	12	7	4	2	1	0
2	RQD	Score	90–100%	75–90%	50–75%	25–50%	<25%		
		Score	20	17	13	6	3		
3	Separation between diaclases	Score	>2 m	0.6–2 m	0.2–0.6 m	0.06–0.2 m	<0.06 m		
		Score	20	15	10	8	5		
4	State of the discontinuities	Length of the discontinuity	<1 m	1–3 m	3–10 m	10–20 m	>20 m		
		Score	6	4	2	1	0		
		Gap	None	<0.1 mm	0.1–1.0 mm	1–5 mm	>5 mm		
		Score	6	5	3	1	0		
		Roughness	Very Rough	Rough	Slightly rough	Undulate	Soft		
		Score	6	5	3	1	0		
		Filler	None	Hard-filled < 5 mm	Hard-filled > 5 mm	Soft-filled < 5 mm	Soft-filled > 5 mm		
		Score	6	5	3	1	0		
Disturbance	Unaltered	Slightly altered	Moderately altered	Very altered	Decomposed				
	Score	6	5	3	1	0			
5	Groundwater	Overall status	Dry	Slightly humid	Humid	Dripping	Flowing water		
		Score	15	10	7	4	0		
Rock Mass Quality									
Grade		I	II	III	IV	V			
RMR		100–81	8–61	60–41	40–21	<20			
Quality		Very Good	Good	Fair	Poor	Very Poor			

F₂: depends on the discontinuity dip (β_j) in the case of planar failure and the plunge (4):

$$F_2 = \tan^2(\beta_j) \tag{4}$$

where β_j is the joint dip.

F₃ is the relationship between the dip of the joint and the dip of the slope. With a higher inclination of the slope, the joints are more exposed and the conditions are less favorable.

F₄ depends on the excavation methods of the slope, whether these are natural erosion processes or blasting techniques.

Table 3. Slope Mass Rating (SMR) classification of slopes. Source: [5].

Adjustment factors for the orientation of the joints (F ₁ , F ₂ y F ₃)						
Case		Very Favorable	Favorable	Fair	Unfavorable	Very Unfavorable
P	α _j - α _s	>30°	30–20°	20–10°	10–5°	<5°
T	α _j - α _s - 180					
P/T	F ₁	0.15	0.40	0.70	0.85	1.00
P	β _j	<20°	20–30°	30–35°	35–45°	>45°
	F ₂	0.15	0.40	0.70	0.85	1.00
T	F ₂	1	1	1	1	1
P	β _j - β _s	>10°	10–0°	0°	0° to -10°	<-10°
T	β _j + β _s	<110°	110–120°	>120°	-	-
P/T	F ₃	0	-6	-25	-50	-60
Adjustment Factor according to the Excavation Method (F ₄)						
Method		Natural Slope	Precut	Soft Blasting	Blasting or mechanical excavation	Poor blasting
F ₄		+15	+10	+8	0	-8
Stability Classes						
Classes		V	IV	III	II	I
SMR		0–20	21–40	41–60	61–80	81–100
Description		Very Poor	Poor	Fair	Good	Very Good
Stability		Totally unstable	Unstable	Partially stable	Stable	Totally Stable
Break		Large breaks through continuous planes or mass	Joints or large wedges	Some joints or many wedges	Some blocks	None
Treatment		Re-excavation	Correction	Systematic	Occasional	None
P: Flat break		α _s : Slope direction		α _j : Joint Direction		
T: Break by rollover		β _s : Dip of the slope		β _j : Dip of the joints		

CSMR

The Chinese method [30] modifies the conventional SMR method by adding two coefficients, ξ and λ, according to Equation (5):

$$CSMR = (\zeta \times RMR) - (\lambda \times F_1 \times F_2 \times F_3) + F_4 \tag{5}$$

where ζ is the slant height factor and, according to [34], is given by Formula (6):

$$Z = 0.57 + ((0.43 \times 80)/H) \tag{6}$$

where H is the slope height in meters, and λ is the factor that describes the control conditions of the discontinuities (Table 4).

Table 4. Discontinuity factor λ (source: [30]).

λ	Condition of Discontinuities
1.0	Faults, long and weak joints filled with clays.
0.9–0.8	Stratification plans, large-scale joints with the presence of water.
0.7	Tightly linked joints and stratification planes

Detachment Susceptibility

To determine the detachment susceptibility of the studied slope, we applied a theoretical–practical approach based on the criteria of experts [26,27,35,36] and the results obtained in its applications.

The considered parameters and the assigned scores are detailed in Table 5.

Table 5. Scores of the main parameters (source: [26,27,35,36]).

Main Parameters	Score Assigned in the Detachment Susceptibility Analysis (DS)
Lithology	Up to 4.0
Geological structure	Up to 4.0
Morphometry and height	Up to 6.0
Discontinuity and key blocks	Up to 6.0
Water	Up to 6.0
Vegetable cover	Up to 4.0
Seismic	Up to 4.0
Weathering Rank	Up to 4.0

Following the method of [27] (modified by [37]), the values obtained for each parameter allowed for the classification of susceptibility into categories ranging from very low to very high (Table 6). This classification has been used by other authors [38–40].

Table 6. Classification of susceptibility.

Susceptibility Category	Detachment Susceptibility Coefficient (DS)	Observations
I	Very low susceptibility (DS < 8.0)	Stable conditions
II	Low susceptibility (DS between 8 and 15)	Stable conditions; monitoring is required
III	Medium susceptibility (DS between 15 and 21)	Predominantly stable conditions; systematic monitoring is required
IV	High susceptibility (DS between 21 and 28)	Potentially unstable conditions
V	Very high susceptibility (DS > 28)	Unstable conditions

Calculation of the Safety Factor

Eight profiles were developed in the slope (Figure 7), considering the different zones in which the slope was divided, its changes of direction, and extension. The safety factor was calculated for each profile using the Morgenstern–Price method [39], choosing for the analysis the lowest result of the safety factor.

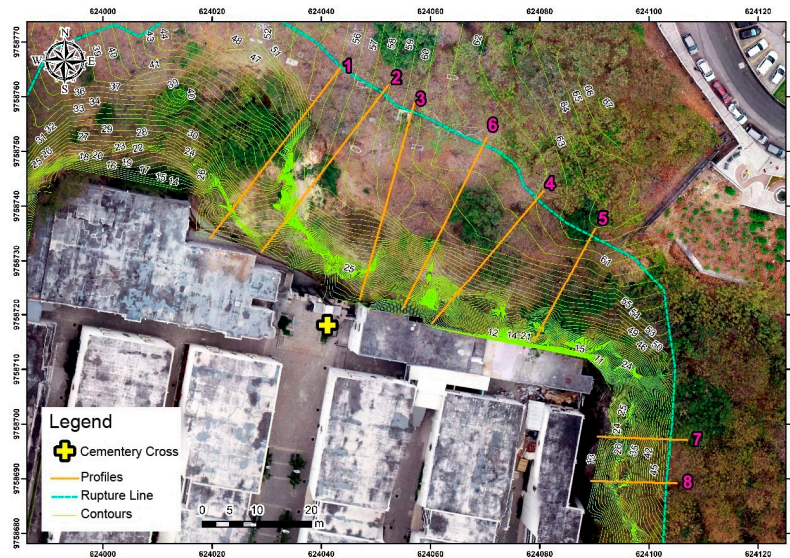


Figure 7. Location map of profiles for calculation of safety factor.

4. Results

4.1. Geology

4.1.1. Stratigraphy

The data collected in the field revealed a stratigraphy of silicified shales of shades of brown-to-gray color with the presence of calcareous material and calcareous sandstone intercalations of beige and dark gray color, with a granulometry that varies from fine to coarse throughout the outcrop and with an approximate thickness of 50 m (Figure 8). The stratification has a strike of N 93° and general dip of 19° SW approximately, with thicknesses of strata that vary from centimetric to decimetric.

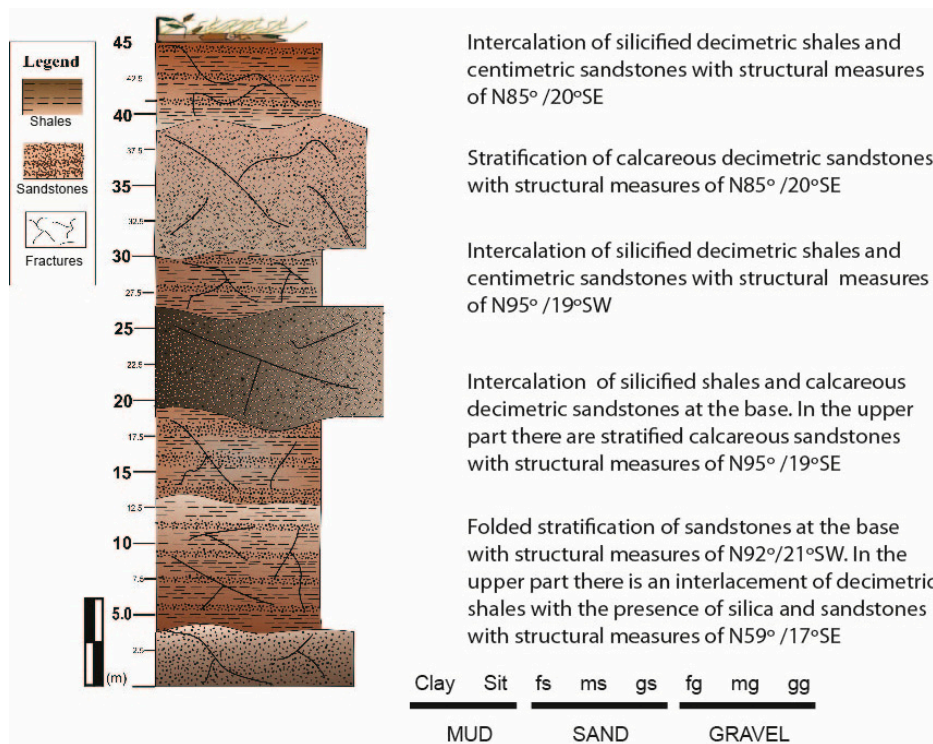


Figure 8. Slope stratigraphic column.

4.1.2. Geomechanical Characterization

The results for each parameter are detailed in Table 7. They were used for the slope stability assessment (Tables 8–11).

Values of compression resistance (Table 7), RQD (Table 8), characteristics of discontinuities (Tables 9 and 10), and water presence (Table 11) intervened in the calculation of stability conditions (Table 12), while the results of density, cohesion, and internal friction angle (Table 7) were necessary to obtain the safety factor value (Table 13).

Physical–Mechanical Properties of Rocks

Table 7. Parameters obtained in laboratory.

9	Rock Type	Description	Physical–Mechanical Properties		Cohesion (MPa)	Internal Friction Angle (°)
			Density (g/cm ³)	Compression Resistance (MPa)		
1	Calcareous sandstone	Dark gray and medium grained	2.30	117.60	18.00	38–40
2	Silicified shale	Brown and fine grained	2.29	107.50	16.60	42–46
3	Silicified shale	Brown and fine grained	2.59	118.50	18.00	40–46
4	Sandstone	Light gray and fine-to-medium grained	2.16	112.20	17.40	36–38
5	Calcareous sandstone	Light gray and fine-to-medium grained	2.38	116.00	14.90	40–42
6	Sandstone	Gray and medium grained	2.32	111.20	15.50	38–40

RQD

Table 8. RQD percentage and classification of rocks for all sectors of the slope.

Zone	Sector	RQD (%)	Classification
1	1	45.27	Poor
	2	51.05	Fair
2	3	55.51	Fair
	4	67.16	Fair
	5	60.50	Fair
	6	71.14	Fair
	7	73.58	Fair
3	8	74.80	Fair
	9	65.12	Fair
	10	66.79	Fair
	11	63.19	Fair

Characteristics of Discontinuities

Table 9. Separation between diaclases for all sectors of the slope.

Zone	Sector	Average Separation (m)	Score
1	1	0.17	8
	2	0.17	8

Table 9. Cont.

Zone	Sector	Average Separation (m)	Score
2	3	0.32	10
	4	0.32	10
	5	0.26	10
	6	0.34	10
	7	0.24	10
	8	0.31	10
	9	0.29	10
3	10	0.26	10
	11	0.38	10

Table 10. Joint conditions for all sectors of the slope.

Zone	Sector	Discontinuity Length (m)	Gap (mm)	Roughness	Filler	Disturbance
1	1					Moderate Score = 3
	2					
	3					
2	4					Very altered Score = 1
	5	3–10 Score = 10	0.1–1 Score = 3	Undulated Score = 1	Soft < 5 mm Score = 2	
	6					Very altered Score = 3
	7					Very altered Score = 1
	8					Moderate Score = 3
9						
3	10				None Score = 6	Very altered Score = 3
	11					

Water Presence

Table 11. Water presence for all sectors of the slope.

Area	Sectors	Water Flow in the Joints	Score
1	1	Dry	15
	2	Slightly humid	10
	3	Flowing water	0
2	4	Humid	7
	5	Dripping	4
	6	Slightly humid	10
	7		10
	8		15
3	9		15
	10	Dry	15
	11		15

4.2. Evaluation of Stability

4.2.1. Stability Conditions

Table 12. Results of the analysis of stability conditions.

Zone	Sector	RMR (%)	SMR (%)	CSMR (%)	Classification	
					SMR	CSMR
1	1	54	44.71	45.45	Fair	Fair
	2	52	41.21	43.45	Fair	Fair
2	3	44	32.93	33.85	Poor	Poor
	4	51	39.93	40.85	Poor	Poor
	5	48	36.93	37.85	Poor	Poor
	6	56	44.93	45.85	Fair	Fair
	7	54	42.93	43.85	Fair	Fair
	8	61	49.93	50.85	Fair	Fair
	9	59	47.93	48.85	Fair	Fair
3	10	65	52.84	54.09	Fair	Fair
	11	65	52.84	54.09	Fair	Fair

4.2.2. Detachment Susceptibility and Safety Factor

Table 13 shows the results of detachment susceptibility obtained for each studied sector together with their qualification according to the reference table (Table 12). The zoning map for the sector and the values obtained from the SF for the different profiles (Figures 9–11) are also displayed.

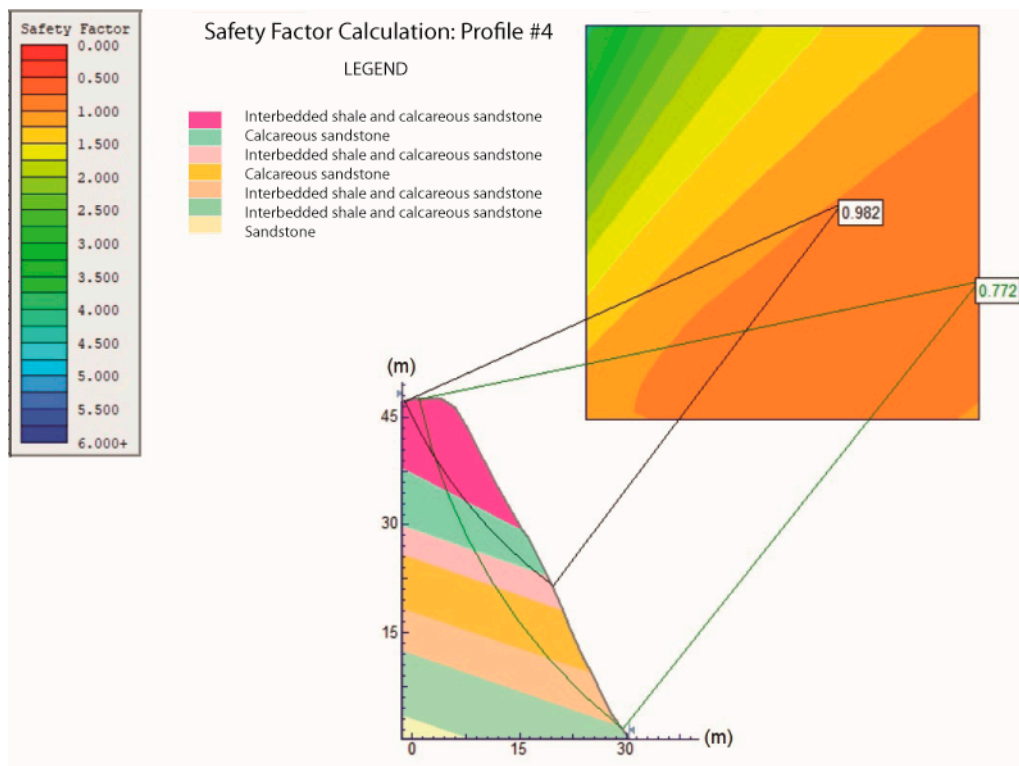


Figure 9. Safety factor calculation for the topographic profile no. 4.

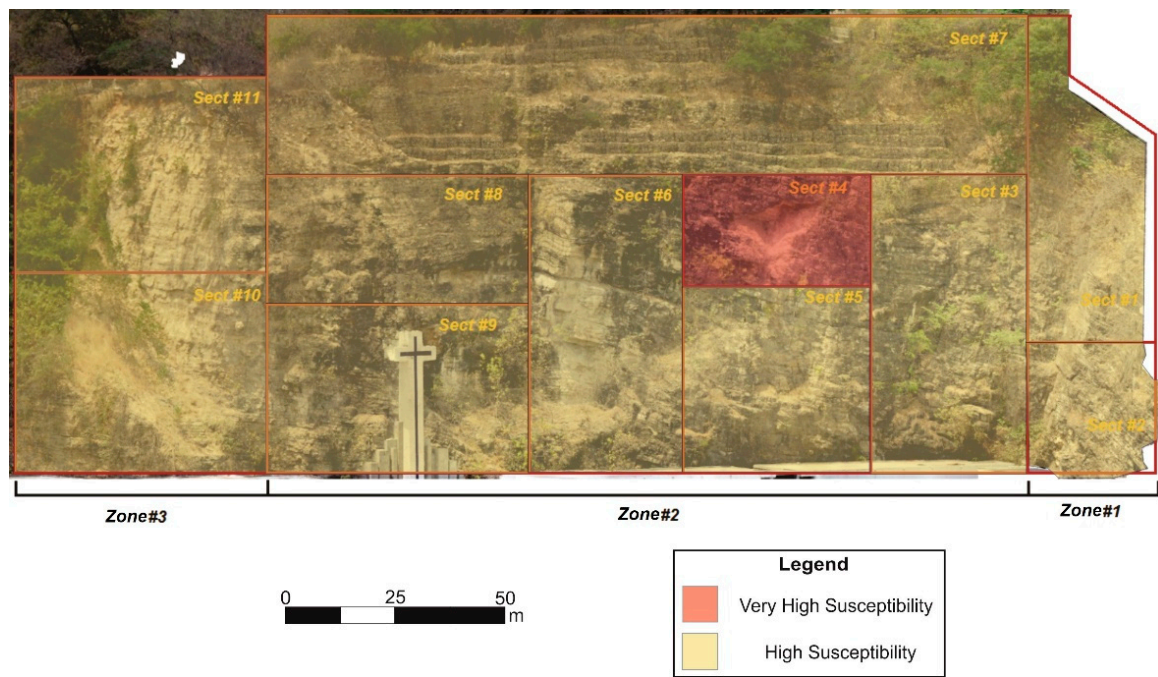


Figure 10. Susceptibility to normal conditions.

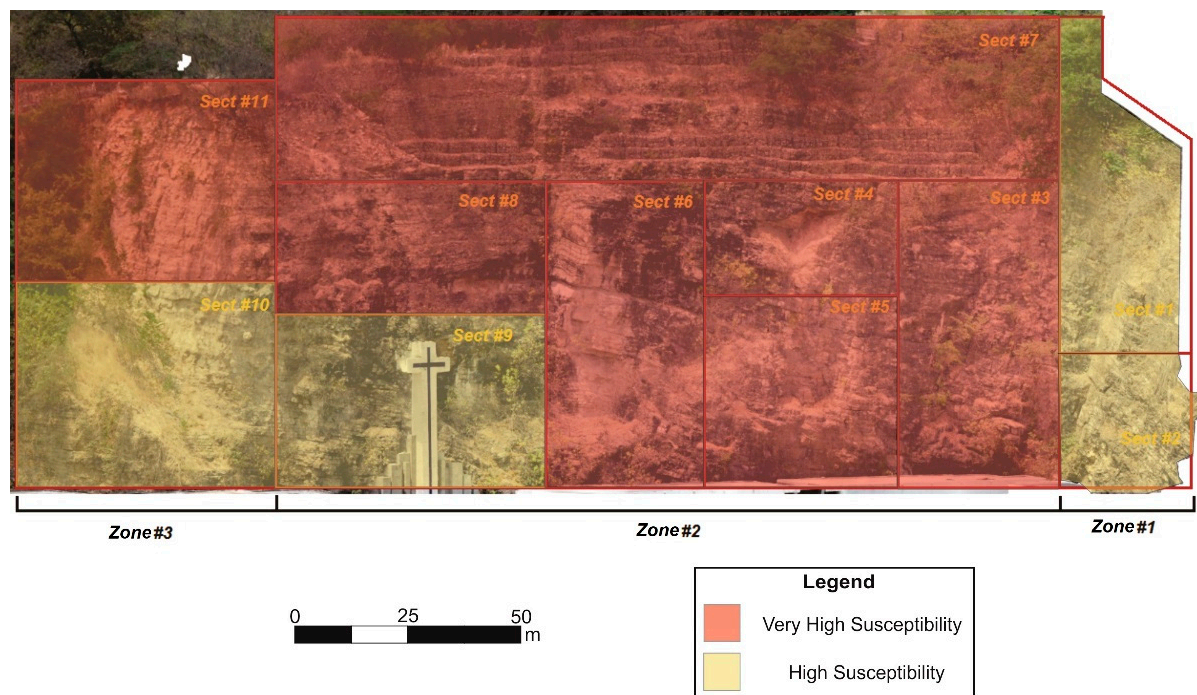


Figure 11. Susceptibility to extreme conditions.

Table 13. Results of detachment susceptibility.

Zone	Sector	Susceptibility: Current Conditions	Susceptibility: Extreme Conditions	Profile	Hypothetical Safety Factor (SF)	Real SF
1	1	High	High	7	0.606	0.996
	2	High	High	8	0.681	0.995
2	3	High	Very High	3	0.677	0.997
	4	Very High	Very High			
	5	High	Very High	4	0.759	0.982
	6	High	Very High	5	0.690	0.989
	7	High	Very High	6	0.725	0.996
	8	High	Very High			
	9	High	High			
3	10	High	High	1	0.831	0.996
	11	High	Very High	2	0.892	0.999

5. Interpretation of Results and Discussion

The lithology of the study area corresponds to the Upper Member of Guayaquil Formation formed by calcareous sandstones and silicified shales in accordance with the information published in [17]. The direction of dip of the strata favors wedge failure.

The similarity of the results obtained with the SMR and CSMR methods allowed us to corroborate the obtained rank of scarp stability. The values are within classes III and IV; that is, a fair-to-poor stability range according to the SMR geomechanical classification table [5]. Sectors 3–5 of the massif have the lowest stability values due to the presence of water, which makes them the most susceptible.

The determined susceptibility was based on a combination of methods that consider various geomechanical parameters described in the literature [26,27,35,36]. This allowed us to establish different zones in the study area according to the conditions of detachment.

A safety factor with a value lower than 1 indicates that the slope is unstable [40]. Two safety factors were calculated for each topographic profile. The first one was a hypothetical SF, which was obtained considering a detachment plane that corresponded to the entire height of the slope. This situation was clearly unrealistic as the slope would fail way before. The second, “real” SF identified the critical point where the instability of the slope might start.

Figure 9 illustrates the above methods. It shows a topographic profile of the slope together with the two detachment surfaces and the corresponding SF values. The hypothetical SF was 0.772, which was only relevant for comparative analysis. The real SF was 0.982, and it represents the current situation of the slope and the surface below which the slope becomes unstable.

The safety factor illustration (Figure 9) corresponded to the topographic profile no. 4 (Figure 7), the average dip of the strata was 19°, and the lithology is shown in Figure 8. The possible detachment surfaces follow lithostratigraphic changes, such as the one around 23 m in the stratigraphic column. This fits the value of the real SF of Figure 9, a fact that offers a relationship between the safety factor values and physical–mechanical properties of the rock.

The applied procedure has been used in similar studies [27] combining traditional techniques of geomechanical characterization [19–24,29,30] with novel techniques, such as the use of drones. The described systematic application of qualitative and quantitative methods for slope stability estimation could be used in other zones with similar problems.

6. Conclusions

The state of the slope was determined by a geomechanical study that included the assessment of stability and detachment susceptibility and the calculation of the safety factor. The obtained results revealed a slope with high failure susceptibility and low stability that requires urgent remediation measures to ensure the integrity of the cemetery, the heritage enclosed therein, and the people who attend the place.

The obtained SMR values were between 32.93 and 52.84, while the CSMR values were found to be between 33.85 and 54.09. The results yielded by the two methods were practically identical and represent a classification of the stability conditions from fair to poor. In Sectors 3–5 of the escarpment, particularly unfavorable stability conditions are present.

The results obtained, considering no precipitation and without seismic influence, yielded very high susceptibility in Sector 4, while the other sectors have a high susceptibility to detachment. When high precipitations were considered together with the possible effect of seismic activity (taking into account that Guayaquil is located in a seismically active area), the detachment susceptibility was found to be very high for Sectors 3–8 and 11 and high for the others.

The safety factor was calculated for eight escarpment profiles, and the value of 0.982 was taken as the most critical one.

The obtained safety factors are in good agreement with the values of detachment susceptibility, which demonstrates the reliability of the obtained results.

7. Recommendations

For a more reliable analysis of stability conditions for high slopes, the CSMR method is recommended because it takes into account the height of the slope and the state of the discontinuities.

The slope should be stabilized using a bolting technique with uniform distribution over the entire surface of the slope (Figure 12), applying gunite (shotcrete) placed in two layers. Due to the conditions of certain parts of the cemetery, the use of metallic meshes is also recommended in order to avoid the detachment of rock fragments.

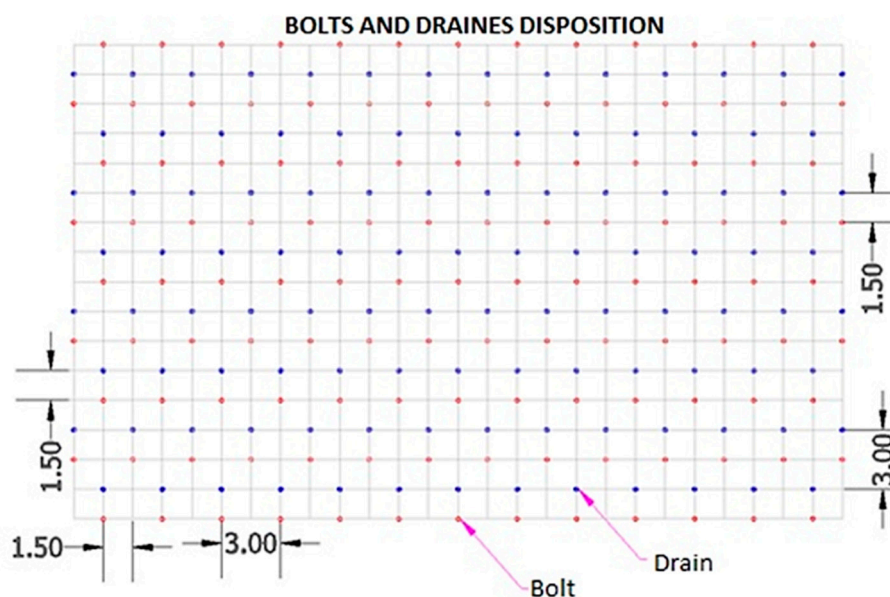


Figure 12. Distribution system of bolts and drains. Red dots represent bolts while the drains are shown in blue. Measures are given in meters.

Author Contributions: Investigation, M.A., G.R., J.B., and E.B.; Supervision, F.M., R.B., and P.C.; Validation, R.B.; Writing—review & editing, J.B., and E.B.

Funding: This research received no external funding.

Acknowledgments: The authors are grateful to ESPOL (Polytechnic University, Ecuador) and IGME (Geological Survey of Spain) for their supporting in this research. Thanks are due to Timea Kovacs for her suggestions. We also would like to thank two anonymous reviewers for their constructive comments and the editorial office for the editorial handling.

Conflicts of Interest: The authors declare no conflict of interest.

Abbreviations

SMR	Slope Mass Rating
CSMR	Chinese Slope Mass Rating
SF	Safety Factor
RQD	Rock Quality Designation
RMR	Rock Mass Rating
F	Factors
λ	Condition of Discontinuities
DS	Detachment Susceptibility Coefficient

References

- De Matteis, Á.; Estabilidad de Taludes. Rosario: Facultad de C.S. Exactas, Ingeniería y Agrimensura, Universidad Nacional de Rosario. 2003. Available online: <https://www.fceia.unr.edu.ar/geologiaygeotecnia/Estabilidad%20de%20Taludes.pdf> (accessed on 25 February 2019).
- Varnes, D.J.; Cruden, D.M. Landslide Types and Processes. Available online: <http://onlinepubs.trb.org/Onlinepubs/sr/sr29/29-003.pdf> (accessed on 29 December 2018).
- Penning-Rowsell, E.C.; Smith, K. Environmental Hazards: Assessing Risk and Reducing Disaster. *Geogr. J.* **1993**, *159*, 349. [CrossRef]
- Kresna, B.N.; Bahagiarti, S.; Purwanto, P. Geology and Slope Stability Analysis using Markland Method on Road Segment of Piyungan-Patuk, Sleman and Gunungkidul Regencies, Yogyakarta Special Region, Indonesia. *Inter. J. Econ. Environ. Geol.* **2016**, *7*, 42–52.
- González de Vallejo, L.I.; Ferrer, M.; Ortuño, L.; Oteo, C. *Ingeniería Geológica*; Prentice Hall-Pearson Educación: Madrid, Spain, 2002; p. 750.
- Pérez, E. *Estabilidad de Taludes*; Canals i Ports Universitat Politècnica de Catalunya: Catalunya, Spain, 2005; p. 61.
- Alpízar, A. *Metodología de Análisis de Estabilidad de Taludes Para Proyectos Viales*; XI Congreso Nacional de Geotecnia: Congeo, Costa Rica, 2012.
- Salazar, D.G. *Diseño de un Plan Piloto Turístico Educativo Sobre el Cementerio Patrimonial de Guayaquil, Dirigido a los Estudiantes de la Escuela Dr. Avellán Vite de 4to a 7mo año de Educación Básica. Licenciado*; Turismo y Hotelería-Universidad de Guayaquil: Guayaquil, Ecuador, 2017.
- Guayaquil es mi Destino. Available online: <http://www.guayaquilesmidestino.com/> (accessed on 23 December 2018).
- Morante, F.E. Las Zeolitas de la Costa de Ecuador (Guayaquil): Geología, Caracterización y Aplicaciones. Ph.D. Thesis, Ciencias-Universidad Politécnica de Madrid, Madrid, Spain, 2004.
- Alemán, A. *Informe Geológico de la Cuenca Progreso*; Informe no publicado para la Compañía Duke Energy: Guayaquil, Ecuador, 1999.
- Núñez del Arco, E. *Geología del Ecuador*; Escuela Superior Politécnica del Litoral: Guayaquil, Ecuador, 2003; p. 275.
- Olsson, A. Tertiary deposits of NO south America and Panamá. 8th Am. Sci. Congr. Washington. *Geol. Sci.* **1942**, *4*, 231–287.
- Benítez, S.B. Estratigrafía de las formaciones Cayo y Guayaquil en la cordillera Chongón Colonche: Hacia una redefinición. *Geocienc. Rev. del CIGMP Guayaquil* **1990**, *3*, 7–11.
- Lopez Coronel, M.C. Análisis Estructural de la Cuenca Progreso- Secuencias Paleógenas. Ph.D. Thesis, Ingeniería en Geología-Escuela Superior Politécnica del Litoral, Guayaquil, Ecuador, 2016.
- Thalmann, H. Micropaleontology of Upper Cretaceous and Paleoceno in Western Ecuador. *Am. Assoc. Pet. Geol. Bull.* **1946**, *30*, 337–347.
- Benitez, S. Évolution géodynamique de la province côtière sud-équatorienne au Crétacé supérieur- Tertiaire. Available online: http://geologie-alpine.ujf-grenoble.fr/articles/GA_1995_71_3_0.pdf (accessed on 29 December 2018).
- Centro de Investigaciones y Proyectos Aplicados a la Tierra “CIPAT”. *Estudios y Propuestas de Estabilización del Talud en el Cerro del Carmen del Cementerio General*; Informe no publicado para la Junta de Beneficencia de Guayaquil realizado por ESPOLTECH E.P.; Guayaquil Charity Board (Junta de Beneficencia de Guayaquil): Guayaquil, Ecuador, 2018.

19. Li, D.; Wong, L.N.Y. The Brazilian Disc Test for Rock Mechanics Applications: Review and New Insights. *Rock Mech. Rock Eng.* **2012**, *46*, 269–287. [[CrossRef](#)]
20. Ma, T.; Peng, N.; Zhu, Z.; Zhang, Q.; Yang, C.; Zhao, J. Brazilian Tensile Strength of Anisotropic Rocks: Review and New Insights. *Energies* **2018**, *11*, 304. [[CrossRef](#)]
21. Akazawa, T. New test method for evaluating internal stress due to compression of concrete: The splitting tension test. *J. Jpn. Soc. Civ. Eng* **1943**, *29*, 777–787.
22. Carneiro, F.L.L.B. A new method to determine the tensile strength of concrete. In Proceedings of the 5th Meeting of the Brazilian Association for Technical Rules, Lisbon, Portugal, 16 September 1943; pp. 126–129.
23. Stagg, K.G.; Zienkiewicz, O.C. *Rock Mechanics in Engineering Practice*; Wiley: New York, NY, USA, 1968; p. 442.
24. Deere, D.U.; Deere, D.W. *Rock Quality Designation (RQD) after twenty years*; U.S. Army Engineer Waterways Experiment Station: Vicksburg, MS, USA, 1988; p. 101.
25. Priest, S.D.; Hudson, S.D. Discontinuity spacings in rock. *Inter. J. Rock Mech. Min. Sci. Geomech. Abstr.* **1976**, *13*, 135–148. [[CrossRef](#)]
26. Suarez, J. *Deslizamientos y Estabilidad de Taludes en Zonas Tropicales*; Instituto de Investigaciones sobre Erosión y Deslizamientos: Bucaramanga, Colombia, 1998; p. 550.
27. Blanco, R. *Estudios y Propuestas de Estabilización del Cerro Las Cabras*; Informe no publicado para la Municipalidad de Durán realizado por CIPAT-ESPOL; Duran Municipality: Duran, Ecuador, 2015.
28. Anbalagan, R.; Chakraborty, D.; Kohli, A. Landslide hazard zonation (LHZ) mapping on meso-scale for systematic town planning in mountainous terrain. *J. Sci. Ind. Res.* **2008**, *67*, 486–497.
29. Romana, M. A geomechanical classification for slopes: Slope Mass Rating: Principles, Practice and Projects. In *Rock Testing and Site Characterization*; Elsevier: Amsterdam, The Netherlands, 1993.
30. Chen, Z. Recent Developments in Slope Stability Analysis. *Inter. Soc. Rock Mech. Rock Eng.* **1995**, *8*, 1041–1048.
31. Romana, M. The Geomechanical Classification SMR for Slope Correction. *Inter. Soc. Rock Mech. Rock Eng.* **1995**, *8*, 1085–1092.
32. Romana Ruiz, M.; Serón Gáñez, J.B.; Montalar Yago, E. *La clasificación geomecánica SMR: Aplicación, Experiencias y Validación*; V Simposio Nacional sobre Taludes y Laderas Inestables: Madrid, Spain, 2001.
33. Bieniawski, Z.T. *Engineering Rock Mass Classifications: A Complete Manual for Engineers and Geologists in Mining, Civil, and Petroleum Engineering*; John Wiley and Sons: New York, NY, USA, 1989.
34. Anbalagan, R. Landslide hazard evaluation and zonation mapping in mountainous terrain. *Eng. Geol.* **1992**, *32*, 269–277. [[CrossRef](#)]
35. Nicholson, D.; Hencher, S. Assessing the Potential for Deterioration of Engineered Rockslopes. Available online: https://www.researchgate.net/publication/209804864_Assessing_the_potential_for_deterioration_of_engineered_rockslopes (accessed on 29 December 2018).
36. Román, A.Q.; Feoli-Boraschi, S. Comparación de la Metodología Mora-Vahrson y el Método Morfométrico para Determinar Áreas Susceptibles a Deslizamientos en la Microcuenca del Río Macho, Costa Rica. *REV GEO* **2018**, *1*, 17–45.
37. Barrantes, G.; Barrantes, O.; Núñez, O. Efectividad de la metodología Mora-Vahrson modificada en el caso de los deslizamientos provocados por el terremoto de Cinchona, Costa Rica. *Revista Geográfica de América Central* **2011**, *2*, 141–162.
38. Sánchez, C.; Sánchez, A. Evaluación de Amenazas Geodinámicas en el Entorno de la Actividad Minera en la Concesión Minera Palacios. Ph.D. Thesis, Escuela Superior Politécnica del Litoral, Guayaquil, Ecuador, 2018.
39. Morgenstern, N.R.; Price, V.E. The Analysis of the Stability of General Slip Surfaces. *Géotechnique* **1965**, *15*, 79–93. [[CrossRef](#)]
40. Melentijevic, S. Estabilidad de Taludes en Macizos Rocosos con Criterios de Rotura no Lineales y Leyes de Fluencia no Asociada. Ph.D. Thesis, Universidad Politécnica de Madrid, Madrid, Spain, 2005.

